SST 空力最適化問題に対する GA と Adjoint 法の比較

佐々木　大輔[*1]、大林　茂[*1]、中橋　和博[*2]

Comparison of GA and Adjoint Method Applied to SST Aerodynamic Optimization

by

Daisuke Sasaki[*1], Shigeru Obayashi[*1], Kazuhiro Nakahashi[*2]

ABSTRACT

Evolutionary algorithm and adjoint method are very promising approaches for aerodynamic optimization. However, there are few reports available for performance comparison of these methods because they fall into completely different methodologies and because code developments are not easy especially for the adjoint method. This paper provides unique comparison results of these methods applied to aerodynamic optimization of a supersonic wing attached to a fuselage. First, an adjoint method was developed based on the unstructured Euler code. The resulting code was applied to aerodynamic wing optimization of a supersonic wing-fuselage configuration. Next, the same optimization problem was solved by an evolutionary algorithm using the same Euler code. The results show that the evolutionary algorithm is able to find a better solution than the adjoint method. However, the results also indicate that multiple evolution process is necessary to obtain a good result.

1. Introduction

CFD techniques have been improved for higher reliability and higher accuracy recently. As a result, CFD has been integrated into aerodynamic optimization. Automated aerodynamic optimization is expected to reduce time and cost of aircraft design.

In the aerodynamic optimization, a gradient-based method and an Evolutionary Algorithm (EA) are often used [1,2]. In the gradient-based method, sensitivity derivatives of the objective function at the initial design point is calculated and the next design point is determined in the direction of the gradient. This process is continued until a local extreme is found. Gradient-based methods can generally obtain an optimal solution with a small number of evaluations. Since only a local optimal solution is obtained by the gradient-based method, many different initial points should be considered to find a global optimal solution. In addition, sensitivity derivatives must be calculated for each design variable. To reduce the number of CFD evaluations to obtain the sensitivity derivatives, Jameson et al. proposed an adjoint approach [3].

In contrast to the gradient-based method, EA is a stochastic method based on the theory of evolution. In this method, only the objective-function value is used to find an optimal solution and it has a possibility of obtaining a global optimal solution. One of the disadvantages is large computational time due to population-based search, but it can be reduced by parallel computing.

EA and the adjoint method are very promising approaches for aerodynamic optimization. However, there are few reports available for performance comparisons of these methods because they fall into completely different methodologies and because code developments are not easy especially for the adjoint method. This paper provides unique comparison results of these methods applied to aerodynamic optimization of a wing-body configuration for a supersonic transport (SST). The SST configuration was designed by National Aerospace Laboratory (NAL) of Japan for the scaled supersonic experimental airplane project [4]. The present design objective is to reduce the drag coefficient at supersonic cruising speed using an unstructured Euler solver.

[*1] 東北大学流体科学研究所　[*2] 東北大学

2. Adjoint Method

The discrete residual vector of the nonlinear flow equations is null for a converged flow field solution of steady problems, which can be written symbolically as

$$\mathbf{R}_i[\mathbf{Q}(\beta),\mathbf{X}(\beta),\beta]=0 \tag{1}$$

where $\mathbf{Q}$ is a flow variable vector, $\mathbf{X}$ is a grid position vector, β is a vector of design variables. Eq.(1) is directly differentiated with respect to β via chain rule to yield the following equation.

$$\frac{d\mathbf{R}}{d\beta}=\left[\frac{\partial\mathbf{R}}{\partial\mathbf{Q}}\right]\left\{\frac{d\mathbf{Q}}{d\beta}\right\}+\{\mathbf{C}\}=0 \tag{2}$$

$$\text{where } \{\mathbf{C}\}=\left[\frac{\partial\mathbf{R}}{\partial\mathbf{X}}\right]\left\{\frac{d\mathbf{X}}{d\beta}\right\}+\left\{\frac{\partial\mathbf{R}}{\partial\beta}\right\}$$

The total derivative of the objective function F is given as follows.

$$\left\{\frac{dF}{d\beta}\right\}=\left\{\frac{\partial F}{\partial\mathbf{Q}}\right\}^T\left\{\frac{d\mathbf{Q}}{d\beta}\right\}+\left\{\frac{\partial F}{\partial\mathbf{X}}\right\}^T\left\{\frac{d\mathbf{X}}{d\beta}\right\}+\left\{\frac{\partial F}{\partial\beta}\right\} \tag{3}$$

One can introduce an adjoint variable vector and combine Eq.(2) and (3). Coefficients of a flow-variable sensitivity vector form the following adjoint equation.

$$\left[\frac{\partial R}{\partial Q}\right]^T \{\lambda\} + \left\{\frac{\partial F}{\partial Q}\right\} = 0 \qquad (4)$$

If one finds the adjoint variable vector λ which satisfies the above adjoint equation, one can obtain the sensitivity derivative of F with respect to β without any information about the flow variable sensitivity vector $\{d\mathbf{Q}/d\beta\}$. This makes the computational cost for the sensitivity analysis independent of the number of design variables. Equation (3) finally becomes to the following form,

$$\left\{\frac{dF}{d\beta}\right\} = \left\{\frac{\partial F}{\partial X}\right\}^T \left\{\frac{dX}{d\beta}\right\} + \left\{\frac{\partial F}{\partial \beta}\right\} + \{\lambda\}^T \{C\} \qquad (5)$$

3. Evolutionary Algorithm

Figure 1 shows the flowchart of EA used in the present study. The following describes genetic operators employed here in brief. The floating-point representation is used in this study. Selection is based on the ranking method [5], and each individual is assigned to its rank according to the fitness value. The following shows the selection probability.

$$prob = c \cdot (1-c)^{rank-1} \qquad (6)$$

Selection probability of rank 1 is represented by c, and c is set to 0.8. To accelerate the convergence, the best and the second best solutions of each generation are preserved to the next generation automatically. Blended crossover (BLX-α) [6] is adopted. This operator generates children on a segment defined by two parents and a user specified parameter α. In this optimization, α is set to 0.5. The disturbance is added to new design variables at a mutation rate of 10%. If the mutation occurs, new design variables are represented as

$$Child1 = \gamma \cdot Parent1 + (1-\gamma) \cdot Parent2 + m \cdot (ran2 - 0.5)$$
$$Child2 = (1-\gamma) \cdot Parent1 + \gamma \cdot Parent2 + m \cdot (ran3 - 0.5) \qquad (7)$$
$$\gamma = (1+2\alpha) \cdot ran1 - \alpha$$

where *Child1,2* and *Parent1,2* denote encoded design variables of children (members of the new population) and parents (a mated pair of the old generation), respectively. The random number *ran1,2,3* are uniform number in [0,1] and m is set to 10% of the given range of each design variable.

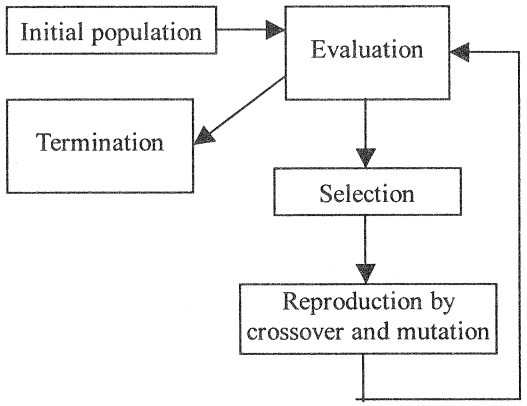

Fig.1 Flowchart of Evolutionary Algorithm

4. Problem Definition

The initial design is taken from SST wing-body configuration designed by NAL as shown in Fig.2. The configuration is composed of wing, body and tail. The main wing shape is designed by the inverse method to achieve a natural laminar flow on the upper surface of the wing.

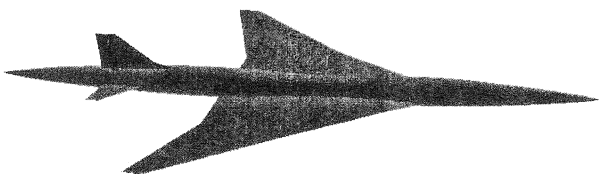

Fig.2 SST configuration (Initial geometry)

4.1 Design Objective

The objective of the present design optimization is defined to minimize drag while maintaining a specified lift C_L^* as

$$F = C_D - \frac{\left(\frac{\partial C_D}{\partial \alpha}\right)}{\left(\frac{\partial C_L}{\partial \alpha}\right)}\left(C_L - C_L^*\right) \qquad (8)$$

where the second term represents the penalty term to prevent reducing the drag by simply reducing the lift. Supersonic cruising Mach number is 2.0 and the target lift coefficient C_L^* is 0.1.

4.2 Design Variables and Grid Modification

In this optimization problem, the main wing shape of the SST configuration is optimized with the fixed wing planform. The wing section geometry is modified adding a linear combination of Hicks and Henne shape functions (Fig.3). 20 Hicks-Henne design variables and one twist angle per a design section are used at five design sections in the spanwise direction as shown in Fig.4. To prevent thinner wing thickness to reduce the drag coefficient, modified thickness must be grater than the initial one at three

chordwise locations (5%, 50%, 80%) for each design section. This corresponds to the following constraint.

$$g_i = Th_{i,design} - Th_{i,initial} \le 0 \qquad (9)$$

where $Th_{i,design}$ is the modified thickness at the i-th constraint position and $Th_{i,initial}$ is the original thickness at the same position. Then the total number of design variables and constraints are 105 and 15, respectively. Upper and lower bounds of design variables and constraints are described in Table 1 where β is a twist angle.

For the movement of interior grid points with a perturbed surface grid, the elliptic partial differential equation method [7] is used. The resulting adjoint solver costs a few times more than the Euler flow solver.

Table 1 Definition of design variables

Definition Location	Airfoil			Twist Angle	
	Number		Constraints	Number	Constraints
η	Upper	Lower	$\beta_L \le \beta_i \le \beta_U$		$\beta_L \le \beta_i \le \beta_U$
0.215	1–10	11–20	$-1.0 \le \beta_i \le 1.0$	101	$-5.0 \le \beta_i \le 5.0$
0.307	21–30	31–40		102	
0.400	41–50	51–60		103	
0.505	61–70	71–80		104	
0.753	81–90	91–100		105	

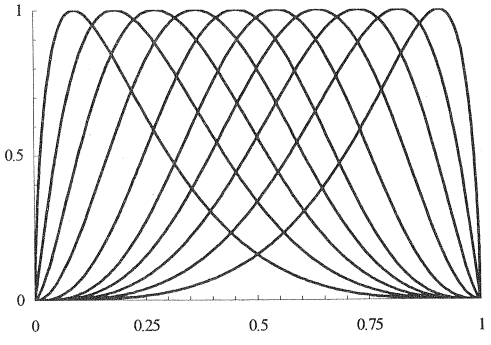

Fig.3 10 Hicks-Henne shape functions

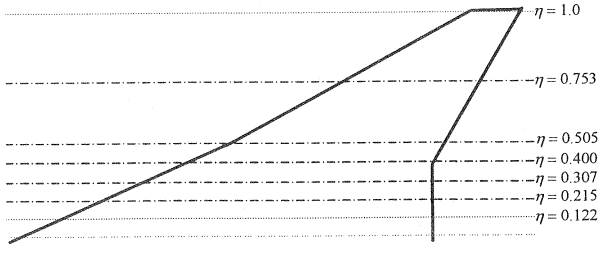

Fig.4 Planform shape and design sections (η=0.215, 0.307,0.400, 0.505, 0.753) for the main wing

4.3 Grid Sensitivity

The grid sensitivity for the vector **C** in Eq.(5) has to be evaluated with respect to each geometric design variable by differentiating the interior grid movement. Since this requires almost the same computational cost with the grid movement procedure, the total computational burden would be substantial as the number of design variables increases.

Figure 5 compares the derivatives of the objective function obtained with and without the interior grid sensitivity information for the wing-body configuration. Since both plots are identical, only the surface grid sensitivities will be used in the following optimization.

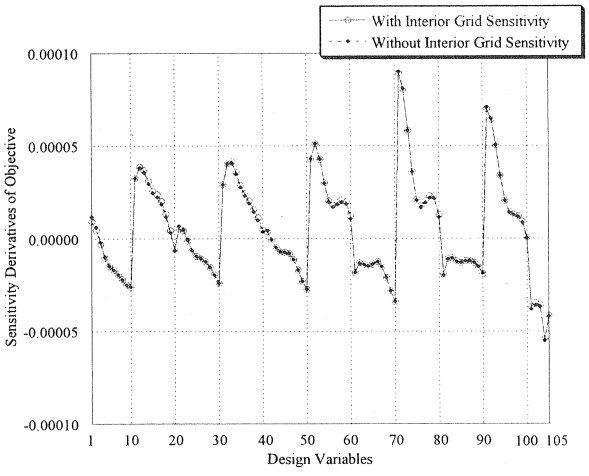

Fig.5 Comparison of sensitivity derivatives with/without interior grid sensitivities

4.4 Aerodynamic Evaluation

The three-dimensional, unstructured Euler code is used to evaluate aerodynamic performance of a wing-body configuration at a supersonic condition. The Euler equations are solved by a finite-volume cell-vertex scheme[8]. Figure 6 shows the NAL SST configuration with the unstructured grid, where the number of nodes and cells are 30,000 and 1,700,000, respectively.

By using the simple *master*(EA)-*slave*(CFD) approach, the present optimization was parallelized on SGI ORIGIN2000 at the Institute of Fluid Science, Tohoku University. The population size used in this study was set to 64 so that the process was parallelized with 64 PEs.

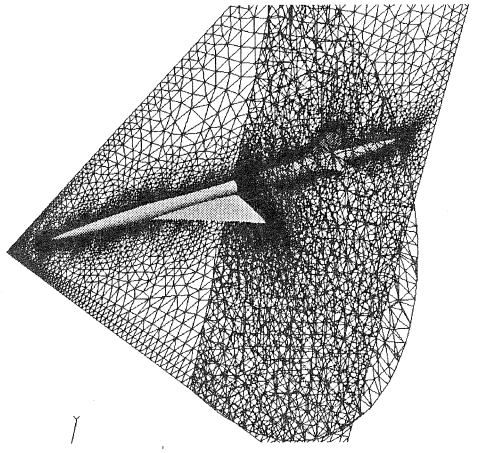

Fig.6 SST wing-body configuration with unstructured grid

5. Results

5.1 Results by Adjoint Method

SQP method [9] was adopted as a design optimizer and the adjoint method was used to supply the sensitivity derivatives. The initial wing geometry shown in Fig.2 was designed for a natural-laminar-flow (NLF) wing and it has good aerodynamic performance at the design condition. SQP optimization was run for three iterations to minimize the objective function while satisfying the geometric constraints. As can be seen in Table 2, the drag coefficient was reduced by about one count retaining the lift coefficient and satisfying the wing thickness constraints. Total evaluation numbers of Euler and adjoint solvers were nine and three, respectively.

5.2 Results by EA

Three different initial populations were first employed for EA. They were generated as follows.

A. All design variables were randomly generated in the design ranges.
B. 50% of design variables were randomly generated in the design ranges and the rest of design variables remained null.
C. 25% of design variables were randomly generated in the design ranges and the rest of design variables remained null.

Examples of three initial populations are shown in Fig.7. If the resulting design does not satisfy the geometric constraints Eq.(9), it is discarded and a new design variables are generated. The same procedure was taken for crossover and mutation during the evolution.

Figure 8 shows the convergence histories starting from three populations A, B and C. A solution better than the initial design was not obtained from these populations in the first 20 generations. The present initialization of design variables distributes the population all over the feasible region. However, because thinner wings generally have lower drag in supersonic flows, good wings are expected to be found at the lower bound of the wing thickness within the feasible region. This kind of prior knowledge about the design space should be incorporated into EA for efficient search.

The idea of island model [10] was then introduced to improve EA's search performance. Emigrants were selected from the final generations of three populations A, B and C. They are considered as a new initial population and the optimization process was restarted. The new population was evolved for 35 generations. The convergence history is summarized in the plots of minimum, average and maximum objective functions as shown in Fig.9. In the figure, objective function values of the initial geometry and the adjoint design are also indicated. In this optimization, the best individual outperforms the initial and adjoint designs at 5 and 23 generations, respectively. Table 2 summarizes their aerodynamic performances. EA design performs slightly better than the adjoint design although EA requires far more computational time.

5.3 Comparison of Design Results

Figure 10 shows a comparison of airfoil shapes among the initial geometry, adjoint design and EA. In this figure, camber lines are found quite different from each other. In addition, EA design is much thinner at 20% chordwise location than the others. EA takes the advantage of the loose problem definition, not only satisfying the constraints. This may cause a problem when placing a wing box for structural integrity. Designers have to define their need precisely and they should doublecheck the optimization result carefully.

In Fig.11, surface pressure distributions are plotted along with the corresponding airfoil shapes. Although the two optimisation approaches are completely different, both configurations are found to utilize the leading-edge suction. This is because of the inviscid flow assumption. The original design, in contrast, intentionally avoided the leading-edge suction to achieve favorable pressure gradient for the NLF wing.

Finally, the distribution of design variables are compared in Fig.12. Design variables are plotted at every spanwise section. For the adjoint result, design variables appear periodic in the spanwise direction. This indicates that the adjoint method cannot utilize the precise geometry representation using a large number of design variables because it is limited to a local search. On the other hand, EA shows more diversity in the distribution. Since it outperforms the adjoint method, it is confirmed to take advantage of having a large number of design variables as a global search.

Table 2 Comparison of aerodynamic performances

	Initial	Adjoint	GA
C_L	0.099962	0.100154 (+0.19%)	0.099978 (+0.02%)
C_D	0.006346	0.006267 (+1.24%)	0.006226 (+1.88%)
L/D	15.75232	15.98111 (+1.45%)	16.05708 (+1.94%)

		β_1	β_2	β_3	β_4	β_5	β_6	β_7	β_8
A	n_1	−0.30	0.25	−0.71	−0.33	−0.68	0.01		
	n_2	−0.77	−0.47	−0.04	0.13	0.87	−0.41		
B	n_1	0.82	0.00	−0.63	0.00	0.00	0.22		
	n_2	0.04	−0.20	0.00	0.75	0.00	−0.92		
C	n_1	−0.44	0.00	0.00	0.15	0.00	0.20		
	n_2	0.00	0.12	0.00	−0.37	0.00	0.00		

Fig.7 Example of initial populations

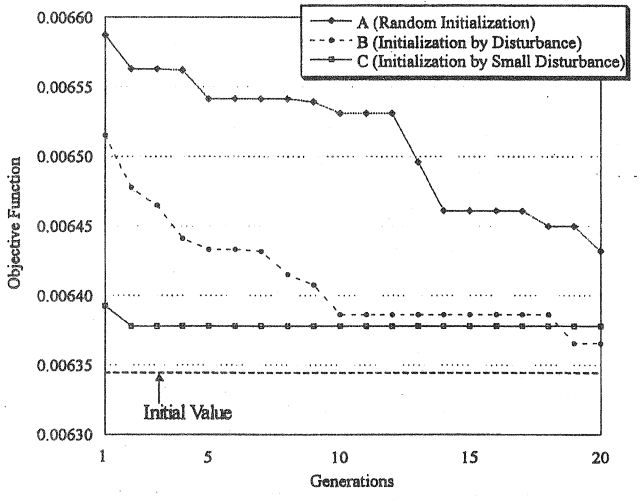

Fig.8 Comparison of convergence histories of minimum objective function values starting from three initial populations A, B and C

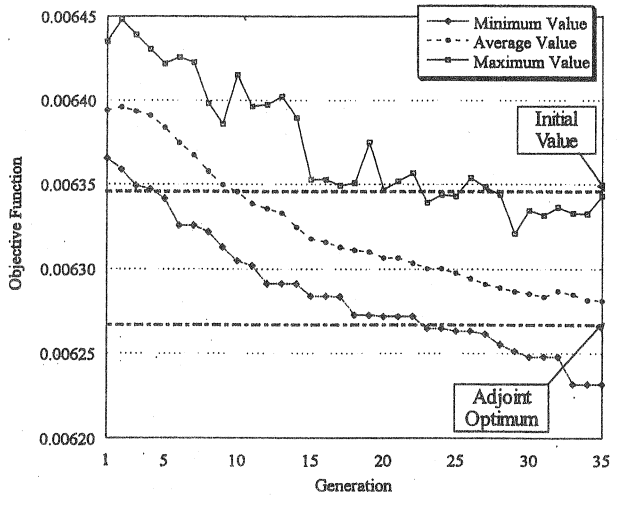

Fig.9 Convergence history of emigrant population

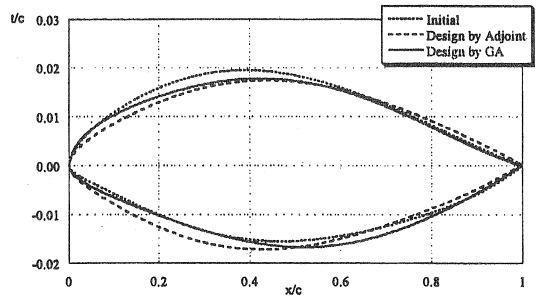

(a) η=0.215

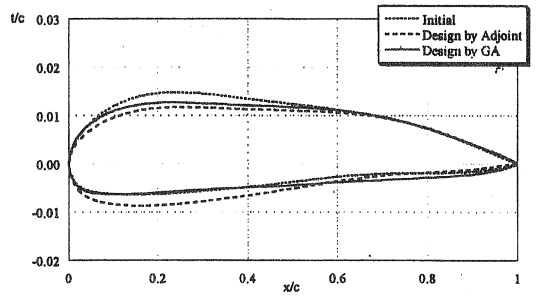

(b) η=0.753

Fig.10 Comparison of airfoil shapes at two spanwise sections

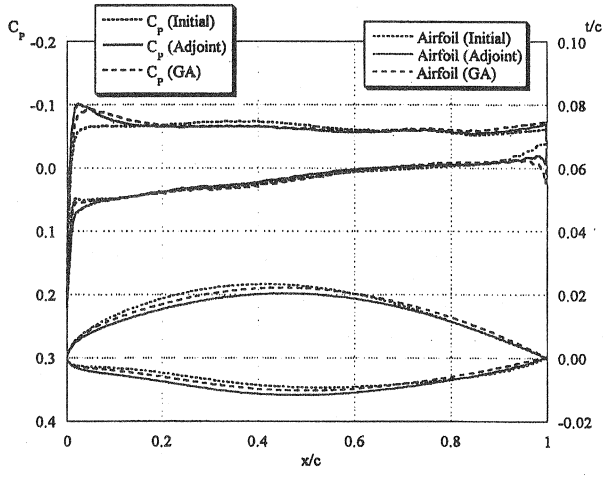

(a) η=0.307

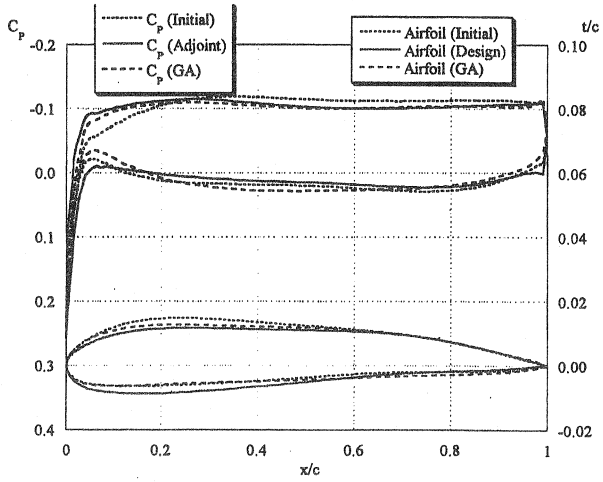

(b) η=0.400

Fig.11 Comparison of Cp distributions at two spanwise sections

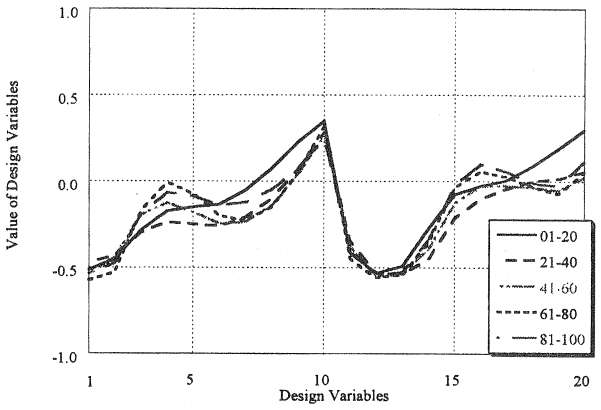

(a) Adjoint design

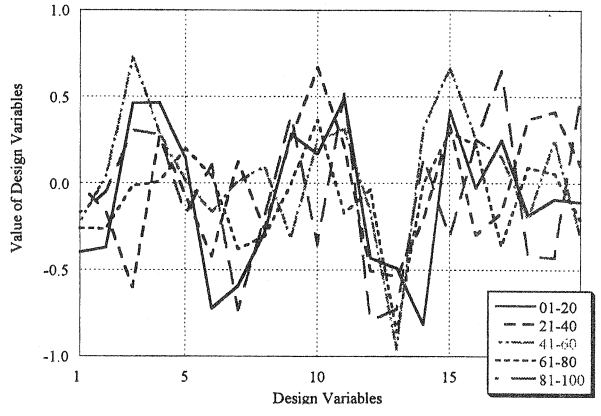

(b) EA design

Fig.12 Distribution of design variables at each spanwise section

6. Conclusion

In this study, SST wing-body configuration was optimized by two different approaches: the adjoint method and EA. The unstructured Euler solver was employed for CFD evaluations. The adjoint method achieved about one count of drag reduction with a relatively small computational cost. On the other hand, EA was able to reduce more drag counts than the adjoint method, but it also required far more computational time. Both designs were found to utilize the leading-edge suction.

Detailed comparison of the resulting optimal designs further revealed the following observations. The adjoint method is computationally efficient, but it is limited to a local search due to the gradient method. The local search cannot fully utilize precise wing definitions using a large number of design variables.

EA requires enormous computational time, but it actually performs a global search, at least better than the gradient method. It enables not only to utilize a large number of design variables, but also to take advantage of loose problem definitions. EA also wastes the search for looking at the entire feasible region, even when the optimal solution is expected near the boundary of the feasible region due to constraints. Therefore, the representation of the optimization problem has to be carefully determined for EA.

Acknowledgement

The present computation was carried out on SGI ORIGINA2000 in the Institute of Fluid Science, Tohoku University. This research was partly funded by Japanese Government's Grants-in-AID for Scientific Research, No. 10305071. The second author's research has been partly supported by Bombardier has been partly supported by Bombardier Aerospace, Toronto, Canada. The authors would like to thank National Aerospace Laboratory's SST design Team for providing many useful data.

References

[1] Reuter, J. and Jameson, A., "Aerodynamic Shape Optimization of Wing and Wing-Body Configuration using Control Theory," AIAA 95-0123, 1995.

[2] Oyama, A., Obayashi, S., Nakahashi, K. and Nakanumra, T., "Transonic Wing Optimization Using Genetic Algorithm," AIAA 97-1854, 1997.

[3] Jameson, A., "Aerodynamic Design via Control Theory," *J. of Scientific Computing*, 3, pp.233-260, 1988.

[4] Sakata, K., "Supersonic Experimental Airplane Program in NAL and its CFD-Design Research Demand," *2nd SST-CFD Workshop*, pp.53-56, 2000.

[5] Michalewicz, Z., *Genetic Algorithms + Data Structure = Evolution Programs*, 3rd revised edition, Springer-Verlag, Berlin, 1996.

[6] Eshelman, L. J. and Schaffer, J. D., "Real-coded genetic algorithms and interval schemata," *Foundations of Genetic Algorithms 2*, Morgan Kaufmann Publishers, Inc., San Mateo, pp.187-202, 1993.

[7] Crumpton, P. I. and Giles, M. B., "Implicit time accurate solutions on unstructured dynamic grids," AIAA 95-1671, 1995.

[8] Sharov, D. and Nakahashi, K., "Reordering of Hybrid Unstructured Grids for Lower-Upper Symmetric Gauss-Seidel Computations," *AIAA J.*, Vol.36, No.3, pp.484-486, 1998.

[9] "Design Optimization Tools USERS MANUAL," Vanderplaats, R&W, Inc., Colorado Springs, 1999.

[10] Loraschi, A., Tettamanzi, A., Tomassini, M. and Verda, P., "Distributed genetic algorithms with an application to portfolio selection problems," *Proc. of the Int. Conf. on Artificial Neural Networks and Genetic Algorithms*, Springer-Verlag, Wien, pp.384-387, 1995.